UNDERSTANDING GOLD-ALKYNE ACTIVATION FROM BOND DISSOCIATION ENERGIES OF GOLD-ALKYNE COMPLEXES

David Gatineau, Denis Lesage, Rodolphe Gueret, Samuel Danladi Mador, Anne Milet, Yves Gimbert

UNDERSTANDING GOLD-ALKYNE ACTIVATION FROM BOND DISSOCIATION ENERGIES OF GOLD-ALKYNE COMPLEXES

David Gatineau,*[a] Denis Lesage,[b] Rodolphe Guéret, [a] Samuel Danladi Mador,[a] Anne Milet,[a] Yves Gimbert*[a]

[a] David Gatineau, Rodolphe Guéret, Samuel Danladi Mador, Anne Milet, Yves Gimbert
Univ. Grenoble Alpes, CNRS, DCM, 38000 Grenoble, France
E-mail: yves.gimbert@univ-grenoble-alpes.fr

[b] Denis Lesage
Sorbonne Université, CNRS, Institut Parisien de Chimie Moléculaire, IPCM, F-75005, Paris, France

Abstract: A detailed approach into electronic effects of ligands on gold-alkyne interactions has been carried out in the gas phase using tandem mass spectrometry. A semi-empirical method coupled to DFT calculations was used to quantify ligands effects on Au-CC bond strength. To this end, the critical energies of 16 [L-Au-hex-3-yne]$^+$ complexes with different L ligands were determined through collision induced dissociation. It was observed that electron-rich ligands destabilize the gold-alkyne bond, whereas phosphites and carbenes strengthened it. The influence of alkyne electronic effects on the gold-alkyne bond has also been studied by dissociation in tandem mass spectrometry on four different alkynes. In an original approach, two successive ion-molecule reactions within the mass spectrometer were used to measure the relative affinity of gold to an alkyne by exchange reactions. The result is that the more electron-rich the alkyne, the stronger the gold-alkyne bond.

Introduction

The activation of alkynes by gold complexes is a widely used method for the formation of C-C bonds under mild conditions, allowing the use of a wide structural variety of organic precursors.[1] From this activation it is possible to engage a broad variety of nucleophiles, which can condense intermolecularly or intramolecularly, leading in the latter case to complex cycloaddition products.[2] The activation of an alkyne by Au(I) results from the electron depletion of the triple bond following its coordination with the metal, making it more reactive towards a nucleophile (Scheme 1a).[3]

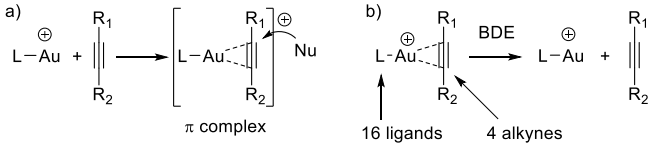

Scheme 1. a) Triple bond activation by gold(I) cationic complexes toward nucleophile; b) influence of both ligand L and alkyne (R_1-≡-R_2) in bond dissociation energy

In this work, we wanted to investigate two aspects that condition/direct the metal-alkyne interaction:
i) The influence of the electronic properties of the ligands L on the ability of Au(I) to increase the electrophilicity for an identical alkyne to which it coordinates;
ii) The influence of the electron-rich or electron-poor nature of the alkyne on the coordination efficiency for the same ligand L.
To study the influence of the ligand L on this activation with Au(I), we need access to an experimental value of an "indicator" that links the electronic properties of L to the ability of the metal, once coordinated to the unsaturation, to increase the electrophilic character of the triple bond.[4] The following assumptions are made: the more cationic the Au, the more its coordination with the unsaturation induces an electronic deficit on the latter, making it more reactive towards a nucleophilic reagent; the stronger the Au-(triple bond) interaction, the higher the dissociation energy of this interaction. It is therefore reasonable to assume that a strong electron-donating ligand will reduce the cationic character of the gold, which will consequently interact less strongly with the unsaturation and thus lower the dissociation energy of the gold-alkyne bond, whereas a less electron-donating ligand will produce an opposite effect (Scheme 1b).

Following a similar line of reasoning, we can expect that in the case of an electron-rich triple bond, the dissociation energy after coordination with gold will be greater than that observed with an electron-depleted triple bond for the same complex L -Au(I).

In 2017, our research teams have already studied ligand effects in gold complexes used in catalysis, involving [L-Au-CO]$^+$ species produced in situ in a homemade mass spectrometer, with CO playing the role of a thermometer ligand.[5] By measuring the bond dissociation energy (BDE) corresponding to the dissociation [(L)Au-CO]$^+$ → (L)Au$^+$ + CO using collision-induced dissociation (CID) in tandem mass spectrometry, we have shown that it is possible to correlate these BDE values with the electronic properties of gold-coordinated ligands. In this work, we have followed the same methodology by experimentally determining the BDEs corresponding to the dissociation [(L)Au-alkyne]$^+$ → (L)Au$^+$ + alkyne as a function of the electronic properties of L and also as a function of the nature of the R1 and R2 substituents on the triple bond (Scheme 1). In 2021, a similar approach was used by Roithova and coworkers in a study to investigate the influence of the structure of unsaturated hydrocarbons coordinated to Au(I)-PPh_3 and Ag(I)-PPh_3 complexes[6] Another study by Gal and coworkers highlighted the influence of alkyne dissociation in JohnPhos(Au$^+$), PPh_3(Au$^+$) and IPr(Au$^+$) complexes.[7]

In this article, we report the study of 16 L-Au(I)-hex-3-yne complexes (**1-16A**) (Scheme 2),[8] the diversity of which lies in the choice of L ligands, by tandem mass spectrometry combined with a theoretical analysis. The experimental procedure employed to measure the BDEs is presented first, followed by a detailed analysis of the results.

The influence of the electronic properties of the alkyne on the dissociation energy of the gold-alkyne bond was carried out on 4 complexes by replacing the hex-3-yne (**A**) with 3 other alkynes (**B-D**). We also present exchange reactions in the gas phase between alkynes according to the electron density present in the unsaturation influenced by the nature of the R^1, R^2 substituents.

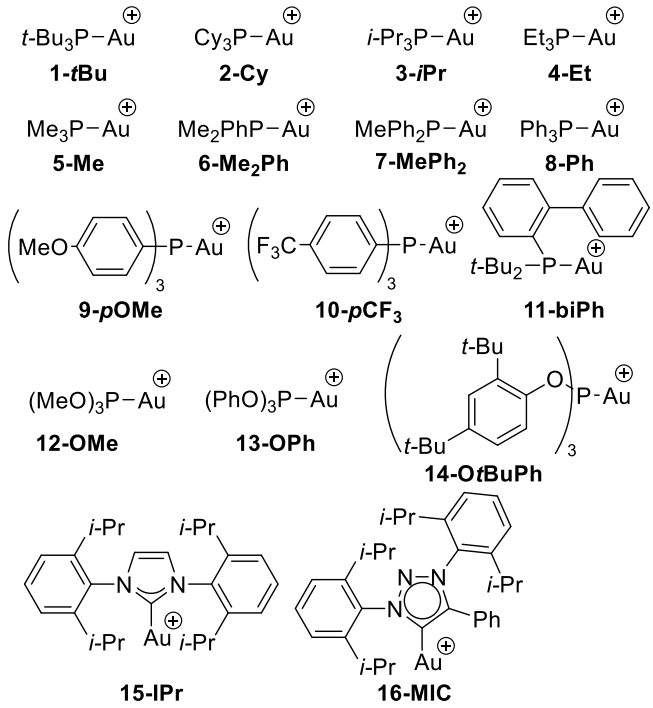

Alkyne = **A** Et—≡—Et

B Me—≡—CO_2Et

C MeO_2C—≡—CO_2Me

D F_3C—≡—CO_2Et

Scheme 2. Gold(I) complexes **1-16** and alkynes **A-D** studied in this work

Results and Discussion

Although the isolation of gold-alkyne complexes has been achieved,[9] the development of a method for obtaining and manipulating these complexes in solution, whatever the ligand carried by the gold, is not straightforward. For our gas-phase study, it would have been possible to form these complexes in the liquid phase by activating [L-Au-Cl] with a silver salt to form L-Au$^+$ ions in solution after precipitating Ag-Cl, then adding an excess of alkyne to obtain the desired complex.[7] However, the reactivity of the complexes formed with methanol - the solvent of choice for species solubility, electrospray

ionization and signal stability - leads to a rapid decrease in the signal intensity of the studied complex. This is why we decided to produce the cationic gold complexes directly in the gas phase, as we had done in our study of gold-carbonyl complexes, through ion-molecule reaction between $[L\text{-}Au]^+$ (**1-16**) and the alkyne (**A-D**) during ion transfer (Scheme 2).[10] Although this process is extremely efficient and very general for stable complexes, it does have one limitation: the vapor pressure of the alkyne must allow it to be introduced directly into the gas phase.
The desired ions were selected in the first quadrupole and then dissociated in the collision cell by collision on argon.

Semi-empirical critical energy measurements on gold-hex-3-yne complexes.

The TCID (Threshold Collision Dissociation) is a robust and well-known mass spectrometric technique allowing the absolute measurement of binding energies under collisional processes.[11] However, it is difficult to implement because it requires a perfect control of the kinetic and internal energy distributions of the precursor ions.[12] Furthermore, the single-collision processes involved are rare for the fragmentation of large systems[13] and comparing the fragmentation of systems of different sizes is still difficult.[14]
Having developed a method enabling the relative critical energy comparison with a good level of confidence of complexes that are extremely different in terms of size (degree of freedom, DoF) and mass, we wished to enlarge this method to gold-alkyne complexes, in our case gold-hex-3-yne **A** complexes with the same ligand series as used in our previous work. Hex-3-yne, A was used for the following reasons: 1) It is perfectly symmetric, so only one conformation is possible when coordinating with gold, and minimal rearrangement is favored by symmetric dissociation; 2) Hex-3-yne is volatile, so formation of the desired complexes is straightforward, regardless of the ligand.
Gold complexes were dissociated under multi-collisional conditions on argon. The loss of hex-3-yne was monitored to obtain the survival yield (SY) as a function of the energy deposited within the collision cell (equation 1).[15]

$$SY = I_{(R+)}/[I_{(R+)} + \Sigma I_{(P+)}] \quad (1)$$

where $I_{(R+)}$ is the abundance of the reactant ions and $\Sigma I_{(P+)}$ is the sum of the abundances of product ions.
The kinetic energy of the reactant ion measured in the laboratory frame (E_{lab}) was converted to the center-of-mass energy E_{CM} to account for the size effect (equation 2).

$$E_{CM} = (M_T/(M_T + M_R))\, E_{lab} \quad (2)$$

Where M_R and M_T are the masses of the reactant ion and neutral target gas, respectively. This center-of-mass energy determines the maximum energy transferred during an inelastic collision.
Sigmoidal survival yield curves were obtained for the 16 chosen complexes (Figure 1a).

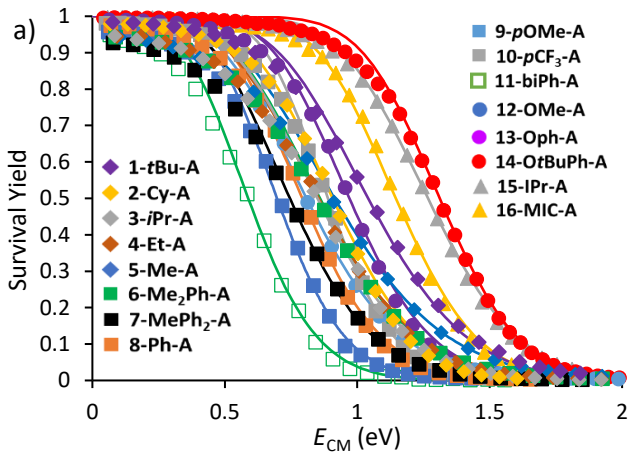

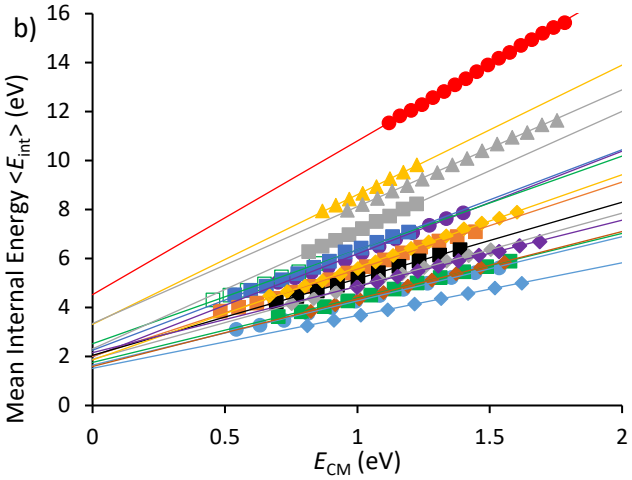

Figure 1. a) Survival yield (markers show experimental data and lines, RRKM modelling) and b) corresponding mean internal energy prior to decomposition (<E_{int}>) of the CID process for the 16 gold-hex-3-yne complexes as a function of the center-of-mass energy (E_{CM}).

As expected, the surviving ion curves are dramatically affected by the size (DoF, from 84 to 372) and mass (from 355 to 925) of the dissociated complexes. To calibrate the amount of energy deposited during the collision,[16] a truncated Maxwell-Boltzmann internal energy distribution model[17] based on transition state theory (RRKM theory)[18] was used and the SY curves were simulated using *Masskinetics* software.[19]

The mean internal energies before fragmentation (<E_{int}>) were calculated and plotted as a function of center-of-mass energy (E_{CM}) for the 16 complexes studied using the sigmoidal curves shown in Figure 1a (Figure 1b). For the truncated Maxwell–Boltzmann internal energy distribution model, we obtained linear correlation of the mean internal energies prior to fragmentation (⟨E_{int}⟩) plotted as a function of center-of-mass energy (E_{CM}). But at low energies, there may be artifacts, such as the presence of other, more fragile forms of low abundance.[5a,14a] Thus, for most complexes, linear regression lies between 10 and 95% of fragmentation.

From the regression lines obtained for the 16 complexes, the slopes and y-intercepts were plotted against the mass of the complexes (Figure 2a) and their number of degrees of freedom (DoF) (Figure 2b), respectively.

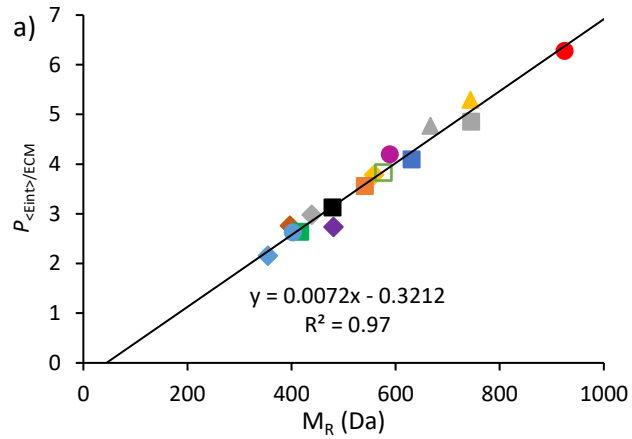

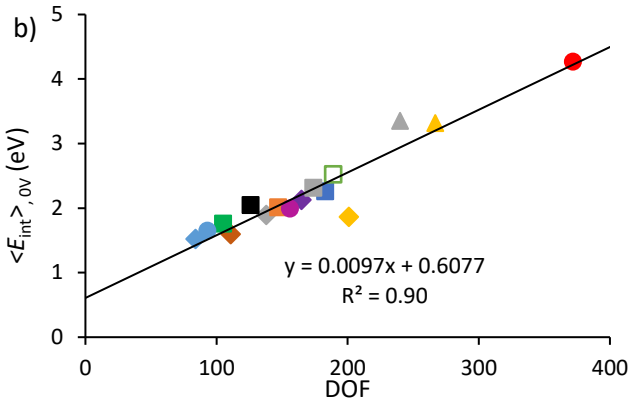

Figure 2. a) Slope of the calibration line ($S_{<Eint>/ECM}$) (from Figure 1b) as a function of the mass of the reactant (M_R) with linear regression (line); b) Mean internal energy at 0 V collision ($<E_{int, 0V}>$) as a function of the DOF with linear regression.

The mass of the complexes correlates well with the slope of the mean internal energies. Although the trend between the number of oscillators as a function of mean internal energy at 0V is weaker, this is observed for all 16 complexes studied, whereas complexes with an alkylphosphine ligand followed a different relationship in the case of gold-carbonyl complexes. It should be noted, however, that the complex with a tricyclohexylphosphine ligand (**2-Cy-A**) is slightly offset from the regression line (yellow diamond, figure 2b).

A general equation has been extracted from the two regression lines to define the relationship between mean internal energy and center-of-mass energy.

$$<E_{int}> = (0.0097\ DOF + 0.6077) + E_{CM}\ (0.0072\ M_R - 0.3213) \quad (3)$$

Equation (3) allows to obtain the deposited mean internal energy $<E_{int}>$ for each complex according to E_{CM}. These $<E_{int}>$ are associated with corresponding characteristic temperatures (T_{char}), which are internal energy distributions prior to decomposition (see SI for details). The critical energies (E_0) (Table 1) for each complex can be determined from these T_{char} vs. E_{CM} values obtained from this calibration and the fitting of the curves (Figure 1).

Table 1. CID experimental critical energy E_0, Computed BDE and selected calculated bond lengths at PBE0-D3BJ/def2-TZVP level.

Complex $[L\text{-}Au\text{-}CC]^+$	E_0[a]	Comp. BDE[a]	Au-P[b] *Au-C*[b]	Au-(CC) [b]	Au(C-C) [b]
1-*t*Bu-A	2.04±0.17	1.91	2.310	2.250/2.253	1.229
2-Cy-A	2.01±0.18	1.87	2.302	2.253/2.254	1.229
3-*i*Pr-A	1.96±0.15	1.95	2.302	2.253/2.254	1.229
4-Et-A	1.97±0.17	2.00	2.291	2.253/2.255	1.229
5-Me-A	2.07±0.21	2.07	2.287	2.253/2.253	1.229
6-Me_2Ph-A	2.03±0.16	2.05	2.290	2.250/2.251	1.229
7-$MePh_2$-A	1.93±0.14	1.99	2.287	2.245/2.248	1.230
8-Ph-A	1.98±0.13	1.95	2.290	2.246/2.249	1.229
9-*p*OMe-A	1.86±0.12	1.81	2.291	2.248/2.251	1.229
10-*p*CF_3-A	2.12±0.11	2.08	2.289	2.246/2.247	1.230
11-biPh-A	1.73±0.11	1.73	2.310	2.240/2.257	1.229
12-OMe-A	2.00±0.19	2.07	2.277	2.261/2.264	1.229
13-OPh-A	2.15±0.15	2.17	2.266	2.241/2.250	1.230
14-O*t*BuPh-A	2.21±0.06	2.20	2.268	2.236/2.245	1.230
15-IPr-A	2.25±0.11	2.38	*2.008*	2.212/2.212	1.231

16-MIC-A	2.16±0.10	2.23	*2.011*	2.211/2.212	1.231

[a] Energies in eV. [b] bond length in Å

By varying the parameters affecting the relative difference between these critical energies (see SI for details), the uncertainties in the critical energies for the 16 gold complexes were estimated. This calibration method has been applied to 16 different complexes. It allows critical energy values to be compared with good confidence in the range of uncertainties. It's worth noting that relative errors between molecules (particularly between similar molecules such as **8-Ph-A**, **9-pOMe-A** and **10-pCF3-A** (which have a triarylphosphine ligand) are much smaller.

Ligand effect on Gold-hex-3yne bond dissociation

To assist in the interpretation of the experimental results, DFT calculation were performed. Calculated bond dissociation energies (BDEs) were performed at the PBE0-D3BJ[20] level of calculation with the def2-TZVP[21] basis set using Gaussian09 D01[22] for geometry optimizations, frequencies and single point energy calculations. Energy decomposition analysis (EDA) were also conducted to gain a better understanding of the nature of the gold-hex-3-yne bond at the BP86-D3BJ/TZ2P level of theory with the ADF package.[23] Relativistic effects were considered via the zero-order regular approximation (ZORA) Hamiltonian.[24] The EDA scheme allows the interaction energy to be divided into four terms resulting to the total interaction energy (ΔE_{int}) as shown in equation (4):

$$\Delta E_{int} = \Delta E_{elect} + \Delta E_{Pauli} + \Delta E_{oi} + \Delta E_{disp}. \quad (4)$$

With ΔE_{elect}, the electrostatic interaction between the unperturbed charge distribution of the fragments, ΔE_{Pauli}, term corresponds to the quantum repulsive Pauli interaction, ΔE_{oi} the covalent component of the bond, accounts for electron pair bonding, charge transfer and polarization and ΔE_{disp}, the D3BJ dispersion correction (Table 2).[25]
Experimental critical energies (E_0) are compared with theoretical calculations (BDEs) (Figure 3a). The BDE is the calculated change in the enthalpy of dissociation reaction at 0 K, while the critical energy represents the difference between the energy of formation of the transition state for dissociation and that of the precursor ion at 0 K. As fragmentation is achieved without reverse activation barriers, these two values are very close and may be considered to be approximately equal.[5a]

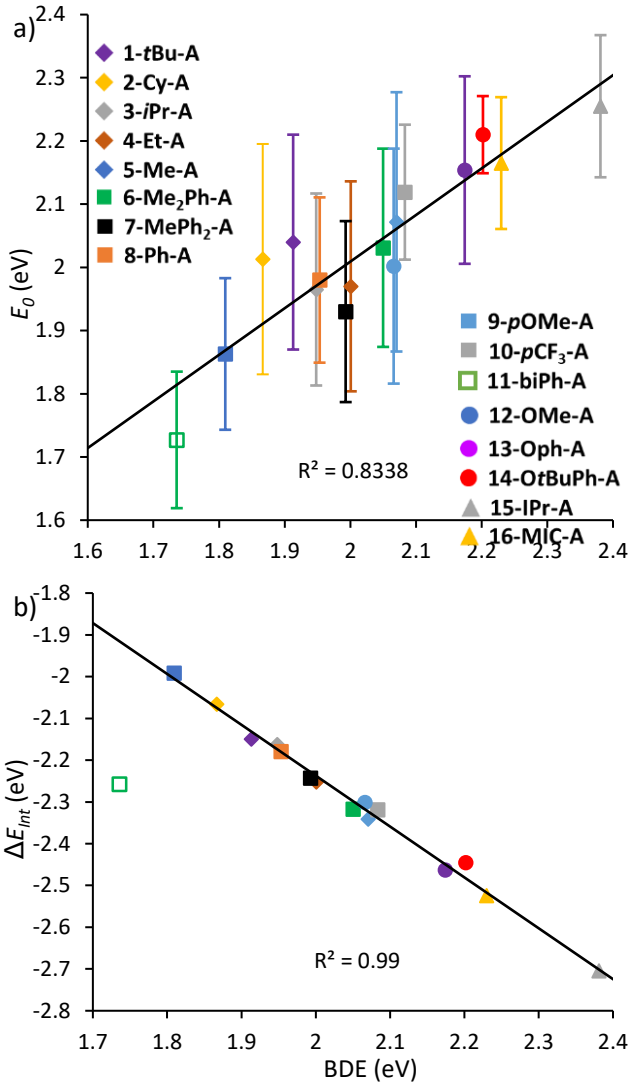

Figure 3 a) Correlation plot between the BDEs and E_0 (values given in Table 1). b) Correlation plot between the BDEs and bond interaction energy ΔE_{int} on the basis of the values given in Table 1.

Although the correlation coefficient is only 0.83 between theoretical and experimental values, there is indeed a correlation between calculated and experimental values. The correlation is very slightly better than in the case of gold-carbonyl complexes (0.81).[5a] What's more, the difference in dissociation energy between the weakest and strongest complexes is relatively small (from 1.73eV to 2.38eV), so even a small error on the strongest complex will result in a significant variation in the slope. The calculated difference between the weakest bond for **11-biPh-A** and the strongest bond for **15-IPr-A** is 0.65 eV. This difference is more pronounced than in the case of the gold-carbonyl complexes (0.51 eV) and the dissociation energies of the gold-alkyne bond are also on average 0.5 eV higher.[5a] This stabilization reflects the greater affinity of gold(I) complexes for hex-3-yne compared with carbonyl.

Figure 3b shows the correlation plot obtained between calculated BDEs and ΔE_{int} from EDA. As expected when fragments are slightly rearranged during dissociation, excellent correlation ($R^2 = 0.99$) is obtained excluding the **11-biPh-A** complex, which undergoes deformation during alkyne dissociation. This case will be examined in detail below. Steric interactions [26] ($\Delta E^0 = \Delta E_{elect} + \Delta E_{Pauli}$) destabilize the Au-alkyne interaction with positive values (Table 2). The presence of strong Pauli repulsion in gold cationic complexes implies destabilization of the gold-alkyne interaction due to steric repulsion.

Table 2. EDA results of the Au-CC bond complexes **1**-**16**[a]

Complex $[L\text{-}Au\text{-}CC]^+$	ΔE_{int}	ΔE_{elect}	ΔE_{Pauli}	ΔE_{oi}	ΔE^0	ΔE_{disp}
1-*t*Bu-A	-2.15	-4.52	5.51	-2.65	0.98	-0.49

2-Cy-A	-2.07	-4.50	5.50	-2.61	1.00	-0.46
3-*i*Pr-A	-2.16	-4.46	5.36	-2.63	0.90	-0.43
4-Et-A	-2.25	-4.43	5.24	-2.65	0.81	-0.41
5-Me-A	-2.34	-4.41	5.12	-2.68	0.71	-0.36
6-Me_2Ph-A	-2.32	-4.46	5.22	-2.68	0.76	-0.39
7-$MePh_2$-A	-2.24	-4.60	5.50	-2.72	0.91	-0.43
8-Ph-A	-2.18	-4.62	5.60	-2.71	0.98	-0.44
9-*p*OMe-A	-1.99	-4.72	5.88	-2.70	1.15	-0.45
10-*p*CF_3-A	-2.32	-4.61	5.51	-2.78	0.91	-0.44
11-biPh-A	-2.26	-4.63	5.76	-2.67	1.14	-0.73
12-OMe-A	-2.30	-4.35	5.13	-2.68	0.77	-0.39
13-OPh-A	-2.46	-4.64	5.62	-2.78	0.98	-0.66
14-O*t*BuPh-A	-2.45	-4.75	5.85	-2.81	1.10	-0.73
15-IPr-A	-2.70	-4.94	5.88	-2.88	0.95	-0.78
16-MIC-A	-2.52	-4.92	5.87	-2.83	0.95	-0.64

[a] Energies in eV.

To support the discussion, the results are analyzed by series.

*[Triakylphosphine-Au-A]$^+$ (**1-5-A**)*

Complexes with a triakylphosphine ligand (**1-5-A**) dissociate with critical energies very close to each other within the uncertainty range, and the theoretical evolution of BDEs is not observed (Cy < *t*Bu < *i*Pr < Et < Me). The PR_3 global ability to increase electron density on a metal by inductive effect of the R group is represented by the electrostatic interaction with Me < Et < *i*Pr < Cy < *t*Bu. However, as mentioned above, the Pauli repulsions overcome the electrostatic interaction and perfectly reflect the steric repulsion of the ligand on the Au-alkyne bond: *t*Bu ≈ Cy > *i*Pr > Et > Me. It appears that the inductive donor effect of trialkylphosphine ligands does not dominate the strength of the gold-alkyne bond, but that steric repulsions are more important. The increase in calculated P-Au bond lengths from 2.287 Å to 2.310 Å for **5-Me-A** and **1-*t*Bu-A** respectively (Table 1, entry 5 and 1 respectively) reflect this steric repulsion due to ligand hindrance.

*[$PMe_{3-n}Ph_n$-Au-A]$^+$ (**5-8-A**)*

For complexes **5-8-A** bearing $PMe_{3-n}Ph_n$ (n = 0-3) ligand, BDE decrease monotonically in the order PMe_3 > PMe_2Ph > $PMePh_2$ > PPh_3 and critical energies follow the same trend, except for **8-A** which is slightly higher than the calculated value. In this series, the electrostatic interaction is stabilized as the number of phenyl substituents on the ligand increases, and this effect is reflected. However, the increase in the π-donor-acceptor ability of phosphine due to the addition of the phenyl substituent is overshadowed by the Pauli repulsion.

*[pX-Ph_3P-Au-A]$^+$ (**8-10-A**)*

The addition of electron-donating or electron-withdrawing substituents in the para position of the triphenylphosphine phenyl allows us to assess the electronic influence on the gold-alkyne interaction, free from interference from steric effects. Experiments and theory clearly show that the more electron-rich the ligand, the weaker the Au-hexyne bond (**9-*p*OMe-A** < **8-Ph-A** < **10-*p*CF_3-A**). As expected, no geometric variations are observed, and the dispersion values are identical for all 3 complexes. Here again, Pauli repulsions dominate the interaction energy, and the complex with the most electron-rich ligand (9) has the lowest dissociation energy.

*[tBu-JohnPhos-Au-A]$^+$ (**11-biPh-A**)*

As mentioned above, the complex bearing the JohnPhos ligand is particularly interesting due to the presence of the biaryl group, which causes deformation during hexyne dissociation and stabilizes the cationic gold complex by π interaction. Compared to similar sized compounds (Table 2, entries 2, 9 and 10) the dispersion term ΔE_{disp} is much higher (Table 2, entry 11). Thus, coordination of the alkyne to gold prevents the biaryl group from stabilizing the cationic gold by π interaction. The shortest distance between biphenyl and gold is 3.1 Å in the **11-biPh-A** complex, while it is 2.4 Å in the **11-biPh** complex and the Au-P-C(biaryl) angle decrease by 12° (from 115° to 103°) after alkyne dissociation (Figure 4).

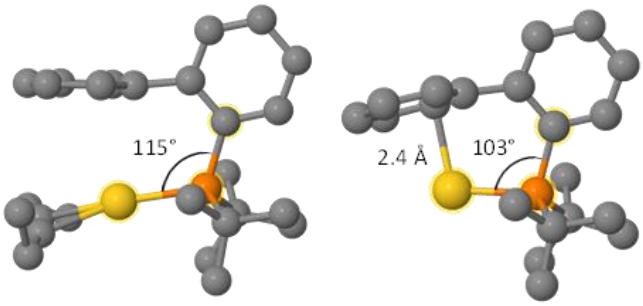

Figure 4. Optimized geometry of **11-biPh-A** (left) and **11-biPh** (right) complexes at PBE0-D3BJ/def2-TZVP level of calculation with the shortest Au-C bond length and the Au-P-C(biaryl) angle (highlighted in yellow and hydrogens are omitted for clarity).

Compared to the **1-tBu-A** complex, complex **11-biPh-A**, in which a tert-butyl substituent has been replaced by a biaryl group, significantly destabilizes the Au-alkyne bond by 0.18 eV thus, having the lowest critical energy of the series. This result can be compared with the work presented by Iacobucci *et al.* who noted a large difference between complexes bearing a triphenylphosphine or *tert*-butyl JohnPhos ligand.[6] In our study, the experimental E_0 difference between the 2 complexes is 0.25 eV, which is in perfect agreement with the reported results.

*[Phosphite-Au-A]$^+$ (**12-14-A**)*

In the series of complexes bearing phosphite ligands, a very good correlation between critical energies and BDEs is found in the order **12-OMe-A** < **13-OPh-A** < **14-O*t*BuPh-A**. The dissociation energy can be linked to the length of the Au-CC bond (the shorter the Au-CC distance, the more stable the dissociation energy) in inverse proportion to ligand size. The results obtained by EDA indicate a reduction of Pauli repulsions (ΔE_{Pauli}) of around 0.7 eV for [phosphite-Au-A]$^+$ **12-14-A** complexes compared with [phosphite-Au-CO]$^+$ complexes, resulting in the stabilization of the Au-CC bond.

*[Carbene-Au-A]$^+$ (**15-16-A**)*

Interestingly, in our previous study, carbenes (**IPr** and **MIC**) stabilized the gold-carbonyl bond by more than 0.31 eV compared with other ligands (phosphines and phosphites).[5a] This stabilization is limited to 0.03 eV between **16-MIC-A** and **14-O*t*BuPh-A**, and 0.18 eV between **15-IPr-A** and **14-O*t*BuPh-A** (Table 1, entry 14 to 16). From the calculated geometries, the Au-CC bond is shorter in the case of complexes with a carbene ligand, but is not stabilized. The electrostatic interaction is identical for MIC and IPr (Table 2, entre 15 and 16), whereas IPr is known to be less of a donor than MIC.[27] Due to the minimal variation observed in the EDA results, interpreting these findings in a rational manner proves to be quite challenging.

Based on all this data, several conclusions can be drawn. On the one hand, a relationship can be established between the electronic environment of the metal and the BDE of the gold-alkyne bond, since the difference observed experimentally between the least stable complex (**11-biPh-A**) and the most stable (**15-IPr-A**) is 0.52 eV. On the other hand, it is possible to classify ligands into general series. Complexes with electron-rich phosphines (complexes **11**, **9**, **2**, **4** and **1**) have the lowest dissociation energies. In contrast, aryl phosphites and carbenes stabilize the gold-alkyne bond (complexes **13-16**). The remaining eight complexes show small variations in dissociation energy, with values ranging from 1.95 to 2.08 eV. The very close values obtained for carbene IPr and phosphites, which exhibit very different reactivities in catalysis,[4a] highlight the importance of not limiting the study to a single reaction step in order to understand all the subtleties of cationic gold-catalyzed reactions.

Influence of electronic properties of alkyne on dissociation of gold-alkyne complexes

Several studies have already been carried out to investigate the influence of the alkyne on the gold-alkyne bond.[6,7] In our study, the hex-3-yne was then replaced by 3 symmetrical and asymmetrical alkynes possessing methyl, CF_3 or ester groups, in order to study the influence of the alkyne on the gold-alkyne bond in the **9-*p*OMe** complex.

After ion-molecule reaction between gold cationic complex generated in the ESI source and the alkyne of interest introduce in the transfer hexapole, the ion of interest is selected and then dissociated to obtain survival yield curves. The collision energy was then converted to center-of-mass energy as before (Figure 5).

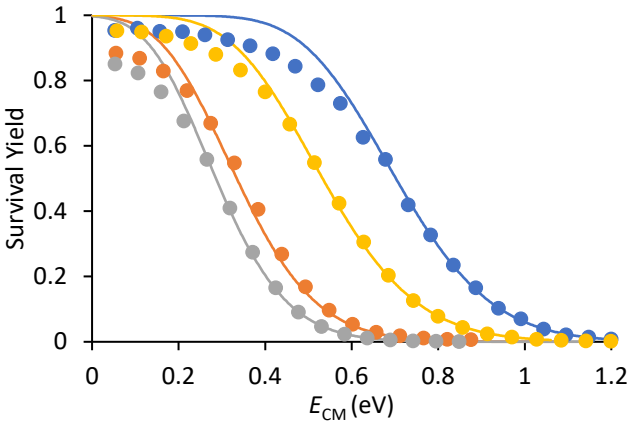

Figure 5. a) Survival yield (dots show experimental data and lines, RRKM modelling) of the CID process for the 4 **9-*p*OMe-A** (blue), **9-*p*OMe-B** (yellow), **9-*p*OMe-C** (orange) and **9-*p*OMe-D** (grey) complexes as a function of the center-of-mass energy (E_{CM}).

In this case, the number of oscillators (183 for the 4 complexes) and the mass of the complexes do not vary significantly (m/z from 631 to 715). Energy calibration is not required for comparison, and the curves for surviving ions/complexes can be directly compared with the energy for 50% dissociation ($E_{1/2}$). The dissociation energy of the complexes increases in the order D < C < B < A for $E_{1/2}$ values of 0.29, 0.33, 0.53, 0.70 eV and the trend is in perfect agreement with the calculated BDE (1.23, 1.33, 1.55, 1.81 eV respectively). In line with literature results, the energy of the Au-C≡C bond is strongly impacted by the alkyne carried by the gold complex, and the more electron-rich the alkyne, the stronger the bond. Thus, hexyne **A**, which has two σ donor alkyl groups, is more strongly bound to gold than ethyl butynoate **B**, which has one electroacceptor ester group. Similarly, alkyne **C** with two ester groups destabilizes the Au-CC bond compared to alkynes **A** and **B**, and alkyne **D** with a strong electron-withdrawing CF_3 group is the least tightly bound to gold.

Exchange reactions

As the affinity of alkynes for gold complexes is strongly linked to their electron content, is it possible to substitute an alkyne with a more electron-rich one directly in the gas phase? In the collision cell, a volatile molecule can be introduced, enabling a second ion-molecule reaction (IMR) to occur in the mass spectrometer. We therefore decided to test whether the alkyne exchange reaction is possible in our experimental setup.
To achieve this, the **5-Me** and **9-*p*OMe** complexes were ionized in the source, then an IMR with the alkynes **B**, **C** and **D** in the transfer hexapole lead to the corresponding complexes. The latter were selected and subjected to a second IMR in the collision cell by introducing hexyne **A** at 10^{-3} mbar (Scheme 3).

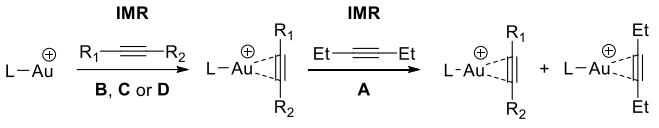

Complex	% Ex
9-*p*OMe-B	88
9-*p*OMe-C	94
9-*p*OMe-D	95

Complex	% Ex
5-Me-B	71
5-Me-C	84
5-Me-D	87

Scheme 3. Exchange reactions realized in homemade triple quadrupole by two consecutive ion-molecule reactions (IMR).

The collision energy was set at 0V to limit dissociation of the complex by collision and maximize reaction time within the cell. The percentage of gold-hexyne ion issue from the exchange reaction (% **Ex**) is calculated identically to the surviving ions (equation 4):

$$\%\ \mathbf{Ex} = I_{(\mathbf{L\text{-}Au\text{-}A})}/[I_{(\mathbf{L\text{-}Au\text{-}A})} + \Sigma I_{(R+)}]*100 \quad (4)$$

where $I_{(\mathbf{L\text{-}Au\text{-}A})}$ is the abundance of the gold-hexyne ions and $\Sigma I_{(R+)}$ is the sum of the abundances of reactants ions.
All the alkynes were exchanged in satisfactory yields (Scheme 3) and the possibility of IMR within the collision cell is therefore validated. Furthermore, at 0V only traces of cationic gold were observed (2% maximum), whereas **L-Au-X** (where **X** = **B**,**C** or **D**) are present up to 29% for the **5-Me-B** complex. This suggests that the energy deposited in the collision cell

is too low to induce complex dissociation, and is in line with the results obtained for the dissociation of gold-alkyne complexes, which undergo few, if any, decompositions at this energy. The formation of the **L-Au-A** complex is indeed the result of an exchange reaction. It is possible to rank the alkynes in order of exchange, with alkyne **D** being the most easily exchanged, followed by **C** and then **B**, as observed above. The difference in critical energies of the gold-alkyne bond observed for complexes **5-Me-A** and **9-*p*OMe-A** is reflected by exchange percentages that are higher for complex **9-*p*OMe**, the least stable, whatever the alkyne associated with gold (Scheme 3, **%Ex**$_{(9\text{-}p\text{OMe-B})}$ = 88 / **%Ex**$_{(5\text{-Me-B})}$ = 71). Moreover, an excellent correlation is observed between the exchange percentages of complexes **5-Me** and **9-*p*OMe** (see supporting information).
This method can easily be used to evaluate the relative affinity of ligands in the gas phase.

Conclusion

In this work, we have taken an in-depth approach to gold-alkyne interactions in the gas phase using a modified triple quadrupole. The influence of the ligand carried by the gold was studied on 16 complexes formed in-situ by ion molecule reaction through experimental determination of the dissociation energy obtained by a semi-empirical method. As the complexes studied are widely different in terms of size and mass, the truncated Maxwell-Boltzmann internal energy distribution model combined with transition state theory (RRKM theory) previously used for gold-carbonyl complexes has been successfully re-used to obtain dissociation energies with good confidence.
Interestingly, the relationships calibrating the amount of energy deposited during the collision (as a function of the mass and degree of freedom of the complex), used for gold-hexyne complexes are identical to those already used for gold-carbonyl complexes, demonstrating the validity of our hypotheses and the reliability of our methodology.
This method is easy to implement when you want to compare molecules with identical dissociation mechanisms and large differences in mass and/or oscillator. However, in order to achieve an effective calibration, it is necessary to perform the study on a sufficiently large cohort to improve its accuracy.
From a chemical point of view, it appears that the most electron-rich ligands - bulkytrialkylphosphine, phosphine with electrowithdrawing substituent or JohnPhos with the biaryl group - destabilize the gold-alkyne bond, while phosphites and carbenes (MIC and NHC) increase the bond's dissociation energy.
The influence of the alkyne carried by the gold was also investigated by varying the electronic environment of 4 alkynes through the addition of electron-withdrawing groups using two tandem mass spectrometry experiment methodologies. We first carried out direct comparisons of dissociation energies at 50% survival yield by CID, then two successive reactions within the mass spectrometer enabled us to carry out alkyne exchange reactions within the collision cell. The decrease in electron density on the triple bond clearly destabilizes the gold-alkyne bond.
These experimental results, although obtained in the gas phase, provide a better understanding of metal-ligand interaction in the case of cationic gold(I) complexes.

Supporting Information

The authors have cited additional references within the Supporting Information.[28]

Acknowledgements

This work was supported by the ANR ManOx project, grant ANR-20-CE07-0007 of the French Agence Nationale de la Recherche and by Labex ARCANE and CBH-EUR-GS (ANR-17-EURE-0003). ICMG (UAR2607) is acknowledged for providing facilities for mass spectrometry analyses and all the computations presented in this article were performed using the Ceciccluster platform of the PCECIC infrastructure. We warmly thank David Martin and Guy Bertrand for their generous gift of the MICAuCl complex.

Keywords: tandem mass spectrometry • reactivity • ion-molecule reaction • organometallic • ligand effects

[1] a) R. E. M. Brooner, R. A. Widenhoefer, *Angew. Chem., Int. Ed.* **2013**, *52*, 11714–11724; b) Z. Lu, G. B. Hammond, B. Xu, *Acc. Chem. Res.* **2019**, *52*, 1275–1288; c) L. Yang, H. Su, Y. Sun, S. Zhang, M. Cheng, Y. Liu, *Molecules* **2022**, *27*, DOI 10.3390/molecules27248956.

[2] a) R. Dorel, A. M. Echavarren, *Chem. Rev.* **2015**, *115*, 9028–9072; b) C. H. Leung, M. Baron, A. Biffis, *Catalysts* **2020**, *10*, 1210.

[3] a) G. Bistoni, P. Belanzoni, L. Belpassi, F. Tarantelli, *J. Phys. Chem. A* **2016**, *120*, 5239–5247; b) J. Gubler, M. Radić, Y. Stöferle, P. Chen, *Chem. - Eur. J.* **2022**, *28*, e202200332.

[4] a) A. Collado, D. J. Nelson, S. P. Nolan, *Chem. Rev.* **2021**, *121*, 8559–8612; b) J. A. Cadge, J. F. Bower, C. A. Russell, *Angew. Chem., Int. Ed.* **2021**, *60*, 24976–24983; c) R. G. Carden, N. Lam, R. A. Widenhoefer, *Chem. - Eur. J.* **2017**, *23*, 17992–18001.

[5] a) D. Gatineau, D. Lesage, H. Clavier, H. Dossmann, C. H. Chan, A. Milet, A. Memboeuf, R. B. Cole, Y. Gimbert, *Dalton Trans.* **2018**, *47*, 15497–15505; b) Measurement of gold-carbonyl bond dissociation were also obtained using blackbody infrared radiative dissociation: D. Gatineau, H. Dossmann, H. Clavier, A. Memboeuf, L. Drahos, Y. Gimbert, D. Lesage, *Int. J. Mass Spectrom.* **2021**, *463*, 116545.

[6] a) P. Motloch, J. Jašík, J. Roithová, *Organometallics* **2021**, *40*, 1492–1502; b) a previous publication was realized with Me_3PAu^+: L. Jašíková, J. Roithová, *Organometallics* **2012**, *31*, 1935–1942.

[7] C. Iacobucci, L. Massi, E. Duñach, P. Burk, J.-F. Gal, *Organometallics* **2021**, *40*, 1642–1653.

[8] Starting material, L-Au-Cl, are commercially available except for a) IPrAuCl preparation see P. de Frémont, N. M. Scott, E. D. Stevens, S. P. Nolan, *Organometallics* **2005**, *24*, 2411–2418; b) MICAuCl preparation see D. R. Tolentino, L. Jin, M. Melaimi, G. Bertrand, *Chem. Asian J.* **2015**, *10*, 2139–2142.

[9] J. Mehara, B. T. Watson, A. Noonikara-Poyil, A. O. Zacharias, J. Roithová, H. V. Rasika Dias, *Chem. - Eur. J.* **2022**, *28*, e202103984.

[10] D. Lesage, A. Milet, A. Memboeuf, J. Blu, A. E. Greene, J.-C. Tabet, Y. Gimbert, *Angew. Chem., Int. Ed.* **2014**, *53*, 1939–1942.

[11] a) M. T. Rodgers, P. B. Armentrout, *Chem. Rev.* **2016**, *116*, 5642–5687 and the references cited therein; b) A. Fedorov, E. P. A. Couzijn, N. S. Nagornova, O. V. Boyarkin, T. R. Rizzo, P. Chen, *J. Am. Chem. Soc.* **2010**, *132*, 13789–13798.

[12] In a previous study using threshold-CID experiments, retarding potential measurements were performed to obtain the kinetic energy distribution in the collision cell of the triple quadrupole: D. Gatineau, A. Memboeuf, A. Milet, R. B. Cole, H. Dossmann, Y. Gimbert, D. Lesage, *Int. J. Mass Spectrom.* **2017**, *417*, 69–75.

[13] For an example of TCID used for large systems see: A. Tsybizova, C. Brenig, C. Kieninger, B. Kräutler, P. Chen, *Chem. - Eur. J.* **2021**, *27*, 7252–7264

[14] For comparison between TCID and multicolisional approach see a) P. Bayat, D. Gatineau, D. Lesage, V. Robert, A. Martinez, R. B. Cole, *J. Am. Soc. Mass Spectrom.* **2019**, *30*, 509–518 and b) M. Regnacq, D. Lesage, M. S. M. Holmsen, K. Miqueu, D. Bourissou, Y. Gimbert, *Dalton Trans.* **2023**, *52*, 13528–13536.

[15] L. Sleno, D. A. Volmer, *J. Mass. Spectrom.* **2004**, *39*, 1091–1112.

[16] K. Vékey, *J. Mass. Spectrom.* **1996**, *31*, 445–463.

[17] a) V. Gabelica, E. D. Pauw, *Mass Spectrom. Rev.* **2005**, *24*, 566–587; b) F. Ichou, D. Lesage, X. Machuron-Mandard, C. Junot, R. B. Cole, J.-C. Tabet, *J. Mass. Spectrom.* **2013**, *48*, 179–186; c) F. Ichou, A. Schwarzenberg, D. Lesage, S. Alves, C. Junot, X. Machuron-Mandard, J.-C. Tabet, *J. Mass. Spectrom.* **2014**, *49*, 498–508.

[18] a) O. K. Rice, H. C. Ramsperger, *J. Am. Chem. Soc.* **1927**, *49*, 1617–1629; b) L. S. Kassel, *J. Phys. Chem.* **1928**, *32*, 225–242; c) R. A. Marcus, *J. Chem. Phys.* **1952**, *20*, 359–364; d) R. A. Marcus, O. K. Rice, *J. Phys. Chem.* **1951**, *55*, 894–908.

[19] *MassKinetics* was used for RRKM modelling: L. Drahos, K. Vékey, *J. Mass. Spectrom.* **2001**, *36*, 237–263.

[20] a) S. Grimme, S. Ehrlich, L. Goerigk, *J. Comput. Chem.* **2011**, *32*, 1456–1465; b) A. D. Becke, E. R. Johnson, *J. Chem. Phys.* **2005**, *123*, 154101; c) E. R. Johnson, A. D. Becke, *J. Chem. Phys.* **2005**, *123*, 024101.

[21] F. Weigend, R. Ahlrichs, *Phys. Chem. Chem. Phys.* **2005**, *7*, 3297–3305.

[22] Gaussian 09, Revision **D.01**, M. J. Frisch, G. W. Trucks, H. B. Schlegel, G. E. Scuseria, M. A. Robb, J. R. Cheeseman, G. Scalmani, V. Barone, B. Mennucci, G. A. Petersson, H. Nakatsuji, M. Caricato, X. Li, H. P. Hratchian, A. F. Izmaylov, J. Bloino, G. Zheng, J. L. Sonnenberg, M. Hada, M. Ehara, K. Toyota, R. Fukuda, J. Hasegawa, M. Ishida, T. Nakajima, Y. Honda, O. Kitao, H. Nakai, T. Vreven, J. A. Montgomery, Jr., J. E. Peralta, F. Ogliaro, M. Bearpark, J. J. Heyd, E. Brothers, K. N. Kudin, V. N. Staroverov, R. Kobayashi, J. Normand, K. Raghavachari, A. Rendell, J. C. Burant, S. S. Iyengar, J. Tomasi, M. Cossi, N. Rega, J. M. Millam, M. Klene, J. E. Knox, J. B. Cross, V. Bakken, C. Adamo, J. Jaramillo, R. Gomperts, R. E. Stratmann, O. Yazyev, A. J. Austin, R. Cammi, C. Pomelli, J. W. Ochterski, R. L. Martin, K. Morokuma, V. G. Zakrzewski, G. A. Voth, P. Salvador, J. J. Dannenberg, S. Dapprich, A. D. Daniels, Ö. Farkas, J. B. Foresman, J. V. Ortiz, J. Cioslowski, and D. J. Fox, Gaussian, Inc., Wallingford CT, 2009.

[23] a) T. Ziegler, A. Rauk, *Theoret. Chim. Acta* **1977**, *46*, 1–10; b) F. M. Bickelhaupt and E. J. Baerends, *Rev. Comput. Chem.,* K. B. Lipkowitz and D. B. Boyd, **2000**, *vol. 15*

[24] E. van Lenthe, A. Ehlers, E.-J. Baerends, *J. Chem. Phys.* **1999**, *110*, 8943–8953.

[25] S. Grimme, S. Ehrlich, L. Goerigk, *J. Comput. Chem.* **2011**, *32*, 1456–1465.

[26] G. Ricciardi, A. Rosa, I. Ciofini, A. Bencini, *Inorg. Chem.* **1999**, *38*, 1422–1431.

[27] a) C. Barnett, M. L. Cole, J. B. Harper, *ACS Omega* **2022**, *7*, 34657–34664; b) N. S. Antonova, J. J. Carbó, J. M. Poblet, *Organometallics* **2009**, *28*, 4283–4287.

[28] M. T. Rodgers, K. M. Ervin, P. B. Armentrout, *J. Chem. Phys.* **1997**, *106*, 4499–4508.